POSITIONING PERFORMANCE OF LOW-COST U-BLOX NEO-M8U MODULE IN URBAN ENVIRONMENT

MICHAL KACMARIK[1], DAVID FOJTIK[2]

[1]Department of Geoinformatics, Faculty of Mining and Geology, VSB – Technical University of Ostrava, 708 00 Ostrava, Czech Republic

[2]Department of Control Systems and Instrumentation, Faculty of Mechanical Engineering, VSB – Technical University of Ostrava, 708 00 Ostrava, Czech Republic

DOI: 10.17973/MMSJ.2023_10_2023080

michal.kacmarik@vsb.cz

Global Navigation Satellite System (GNSS) positioning is nowadays used for many applications, including navigation of various man-drived or autonomous vehicles and pedestrians. As a significant part of these activities take place in cities or other environments which are not favourable for GNSS signal transmission, there is an option to improve the quality of positioning in them by combining the GNSS with other technologies. A fusion with inertial measurement units is probably the most common. The main objective of this paper was the evaluation of low-cost u-blox NEO-M8U module in kinematic positioning. Despite the module is primarily aiming on automotive industry, it was tested for a performance in low speed scenarios. The fusion mode combining input from a single-frequency multi-GNSS receiver and inertial unit was initialized and firstly calibrated on a standard passenger car and lately tested on a remotely controlled small vehicle. In a set of testing drives on three individual routes with a speed of motion around 5 km/h, the accuracy of horizontal position of the u-blox M8U module was in 35% of all measurements better than 1 m and in 84% better than 3 m.

KEYWORDS

GNSS, positioning, untethered dead reckoning, low-cost, urban environment

1 INTRODUCTION

Global navigation Satellite System (GNSS) technology is being commonly used for localization and navigation in a broad list of industry sectors. GNSS receiver has become a natural part of smartphones, mobile robots, transport vehicles and various other devices. In relation with Industry 5.0 [Maddikunta 2022] and smart cities [Javed 2022], we will see a growing amount of applications utilizing robotic systems in upcoming years. Many of them will depend on a robust and sufficiently accurate information about the system absolute localization. Still, positioning of all these devices, vehicles and also pedestrians will often need to be realized in places which are not favourable for GNSS signal transmission. Urban environments are typically full of buildings and various other objects causing either a complete blockage of signal or leading to significant multipath effects. Natural environments with a dense vegetation cover can be comparatively problematic. When using only GNSS technology in these places, the quality of positioning can significantly decrease or may even fail completely. There exist several ways how to reduce or overcome this issue. In vehicular applications, GNSS is most often fused with inertial navigation system (INS) [Aggarwal 2010]. Three integration strategies exist: loosely-coupled [Solimeno 2007], tightly-coupled [Petovello 2003] and ultra-tightly-coupled [Abbott 2003, Feng 2013]. Commercial products are usually based on the first two mentioned integration architectures. Their comparison and assesment was provided e.g. by [Agrisano 2012] or [Falco 2017]. [Toledo-Molero 2007] and [Park 2008] firstly presented results of GNSS/INS fusion for automotive applications in marketable conditions. A combination of GNSS and INS can be further supplemented with odometry, therefore by a measurement of travelled distance realized by wheel ticks [Kubo 2016]. GNSS/INS fusion is commonly found named as untethered dead reckoning (UDR), while GNSS/INS/odometry fusion as automotive dead reckoning (ADR). Besides INS and odometry, data from following sensors can help to enhance positioning quality of a ground vehicle: monocular, stereo or depth map cameras [De Gaetani 2019, Li 2019], Light Detection and Ranging (LiDAR) [Dietmayer 2005, Gao 2015], barometer [Chiang 2020] or visual lane marking detector [Vivacqua 2017].

For outdoor localization and navigation of pedestrians, a fusion of GNSS and INS is applicable as well as shown by [Pany 2009, Le Scornec 2017, Basso 2020]. Another way to improve GNSS positioning for pedestrians in urban environments is the 3D-mapping-aided GNSS technology which integrates the 3D model of surrounding buildings to predict visibility of satellites or even to predict a reflecting path of the signal and its delay [Hsu 2016, Groves 2019].

With advances in technology and efforts to make positioning and navigation more accessible, low-cost mass-market positioning modules has started to be widely accesible since the beginning of the millennium. A few companies are offering all-inclusive commercial low-cost positioning modules nowadays. They are typically based solely on GNSS, or on a combination of GNSS/INS or GNSS/INS/odometer technology. Although the first generations of low-cost modules were using single-frequency GPS/GNSS receivers, dual- and multi-frequency solutions have appered on the market since 2017. In terms of INS, micro-electro-mechanical-system (MEMS) units are implemented in low-cost solutions [Shaeffer 2013].

Low-cost positioning modules of the u-blox company are widely used in scientific works. [Odolinski 2017, Garrido-Carretero 2019, Hamza 2021, Wielgocka 2021] tested u-blox GNSS modules in static land-surveying scenarios. In the former two studies, single-frequency modules (NEO-M8T, NEO-8MP) and well-established Real-Time Kinematic (RTK, [Teunisen 2017]) technique was utilized. In the latter studies, a dual-frequency receiver ZED-F9P was used with undifferenced Precice Point Positioning (PPP, [Zumberge 1997]) or RTK technique. Modern module ZED-F9P and RTK technique was tested also by [Janos 2022], this time in kinematic scenarios. Results of all five studies showed that low-cost devices can achieve a competitive positioning performance compared to geodetic grade receivers, especially when connected to high quality antennas. Another example of low-cost u-blox modules application can be found in displacement and landslide monitoring as shown by [Biagi 2016, Notti 2020, Šegina 2020].

Although land-surveying and landslide monitoring was mentioned in the previous paraghraph, the main target area of the low-cost positioning modules is the automotive industry and transportation in general. Therefore, there is a considerable amount of scientific works devoted to testing existing low-cost devices, finding ways to improve quality of their output or developing own solutions integrating various low-cost electronics. [Rademakers 2016] developed a tool for PPP technique with low-cost GNSS receivers and tested it in various scenarios with a single-frequency u-blox NEO 7P GPS receiver. While they were able to reach 0.5 m accuracy in open areas, it degraded down to 3 m under challenging urban conditions. [Lyu 2020] proposed GNSS observation weighting scheme based on support vector machine (SVM) signal classifier to improve kinematic positioning in urban unvironments. In vehicular tests their solution with low-cost single-frequency u-blox M8T GNSS receiver was reported to even outperform built-in RTK solutions of multi-frequency receivers u-blox F9P and Trimble BD982. SVM signal classifier was also applied by [Xu 2020], in this case to determine satellite visibility in urban areas. Its performance was validated with single-frequency u-blox M8T receiver in static positioning.

[Zhao 2016] presented a real-time sliding-window estimator which tightly integrates differential GPS and inertial measurements for a vehicle localization and navigation. Using a low-cost single-frequency GPS receiver they demonstrated a decimeter level of accuracy in urban environment. [Li 2017] developed a tightly-coupled integration of multi-GNSS single-frequency RTK and MEMS grade INS and assessed it with a Novatel OEM4 receiver. Lately, they advanced their solution with outlier-resistant ambiguity resolution and Kalman filtering approach and validated it with a Trimble BD982 receiver [Li 2018]. In their vehicular tests in an urban environment, the single-frequency multi-GNSS RTK/INS integration outperformed dual-frequency multi-GNSS RTK solution in accuracy and allowed obtaining high-accuracy positioning in the presence of GNSS observation outages. [Gao 2018] proposed a multi-sensor fusion system consisting of multi-GNSS PPP, several low-cost inertial sensors and an odometer and tested various variants of technology fusions with land-borne vehicle. According to the results, the performance of PPP was considerably improved by introducing INS and odometer. Recently, [Kaczmarek 2022] presented a loosely-coupled integration of low-cost sensors (u-blox ZED-F9P GNSS receiver, xsens MTi-7 INS, odometer) and evaluated it in scenarios simulating work of an autonomous lawn mower. Their goal was to develop a solution with price under 1500 USD allowing a precise positioning with an accuracy better than 0.05 m in all terrain conditions. Further examples of scientific works focusing on low-cost GNSS/INS or other sensor fusion for vehicle localization and navigation in urban environments can be found in [Niesen 2018, Gonzalez 2019, Feng 2020].

In this paper, we have assessed a positioning performance of a standard low-cost GNSS/INS u-blox NEO-M8U module in an urban environment. Unlike most of the abovementioned studies, our work is based on scenarios corresponding to a movement of a pedestrian or a low speed (robotic) vehicle which are expanding with the development of battery-powered devices. In order to put UDR fused positioning into operation, the NEO-M8U module must undergo an initialization and calibration drive including periods during which the vehicle is stationary and when it is moving [u-blox 2021]. Since speeds exceeding 40 to 50 km/h are necessary in this procedure, the module is directly aiming on an automotive industry. Our goal was to put the module into UDR mode on a standard passenger car and then evaluate its performance in abovementioned low speed scenarios on another small vehicle. According to our findings, no similar assesment was so far presented. Since the NEO-M8U module is fully independent of any external data as e.g. real-time corrections needed by the GNSS RTK technique, it ensures an easy implementation and operation in any application. Yet we found only a single publication that utilized this module: in [Feng 2020] its internal solution was used as a reference for a comparison with deeply-coupled integration of GNSS and INS developed by the authors and tested in a passenger car.

The paper is organized as follows: in Section 2, a description of tested devices, data collection and methodology of evaluation is given. All obtained experimental results are provided and discussed in Section 3. Conclusions are drawn in Section 4.

2 MATERIALS AND METHODS

In this section, information about tested devices, data collection and processing and methodology of results assessment are provided.

2.1 *Tested devices*

The main evaluated device was the u-blox NEO-M8U module (https://www.u-blox.com/en/product/neo-m8u-module) which combines a single-frequency multi-GNSS receiver and an onboard MEMS inertial unit using a tightly-coupled integration. To be more specific, the u-blox EVK-M8U-0-12 evaluation kit was used in this study which implements the abovementioned positioning module in a user-friendly solution. Signals of GPS, GLONASS, Galileo, BeiDou satellites can be tracked by the device and any dual constellation combination is supported. In terms of triple constellation, either GPS+GLONASS+Galileo or GPS+GLONASS+BeiDou can be used. Signals from QZSS and SBAS augmentation systems can be added to any selected constellation. In the performed tests, the triple constellation GPS+GLONASS+Galileo was utilized while mentioned augmentation systems were kept activated. The original u-blox active patch antenna was connected to the module.

We were also interested in how reliably pedestrian movement can be tracked using GNNS receivers in common smartphones. We thus extended the study further, adding a standard smartphone Samsung A41 running on Android operational system. Similarly to the evaluated u-blox module, the smartphone is equipped with a single frequency multi-GNSS receiver supporting GPS, GLONASS, Galileo and BeiDou signals. During the testing data collection, position of the smartphone was computed and recorded with the freely available UltraGPSLogger application in version 3.186 (https://play.google.com/store/apps/details?id=com.flashlight.ultra.gps.logger&hl=cs&gl=US&pli=1). This application uses Single Point Positioning with code measurements and performs an epoch-wise optimization of the estimated position using a Kalman filter, which leads to a smoothing of the recorded routes. Since the smartphone is based on a different hardware and software, its inclusion does not allow a proper evaluation of the level of benefit of using a fusion of GNSS and INS (u-blox module) compared to GNSS only solution (smartphone). Still, it can provide an idea of positioning performance reached by such a device under tested scenarios.

For the possibility of testing positioning devices in a low-speed kinematic mode, the platform of a remote-controlled (RC) four-wheeled off-road vehicle was used. All necessary equipment was installed on the vehicle. These were the EVK-M8U evaluation kit with GNSS antenna, Samsung smartphone, minicomputer with a display, power bank and an outdoor camera for recording the data collection drives. Figure 1 shows the described platform. GNSS antennas of both the u-blox module and the smartphone were placed only about 0.3 m above the ground.

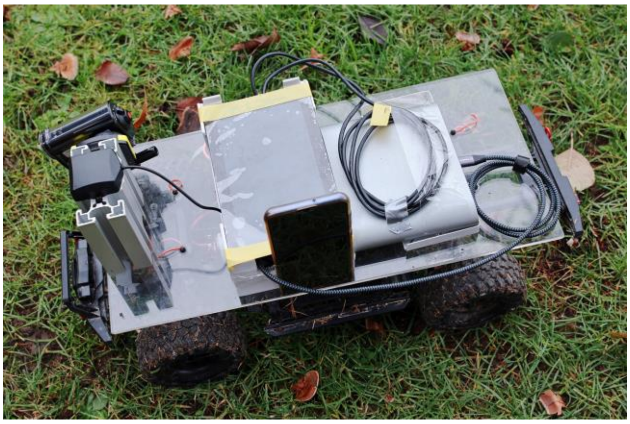

Figure 1. RC vehicle used for the testing drives with installed positioning module and other equipment. The u-blox NEO-M8U module was fixed below the display of minicomputer.

As already mentioned in the previous section, the u-blox NEO-M8U module requires an initialization and calibration in order to start providing the combined UDR positioning. In the first stage, mount alignment angles of the module with respect to the vehicle frame must be given. This can be done either manually by the user, or automatically detected by the module itself during an initialization drive. The latter option was utilized in the presented work. During the initialization drive, also all other unknown parameters required for the fusion are estimated. After the initialization phase, the module enters the fusion mode and further fine calibrates all the necessary parameters. The initialization and calibration procedure is based on prolonged driving (module movement) according to scenarios defined in the receiver specification, which includes driving at a speed of at least 50 km/h, making a series of multiple turns with an angle greater than 90 degrees, some stops, etc.

Since the used RC vehicle does not allow to reach the required speed of movement, the initialization and calibration drive was realized using a passenger car, where the Plexiglas plate with all the devices was fixed on its roof. The orientation of the plate on the roof of the vehicle fully corresponded to the orientation of the plate on the RC vehicle, therefore this solution did not cause any mismatch of the mount alignment angles.

2.2 Experimental setup, data collection

Assessment of the positioning performance of the tested devices was performed on three individual routes with various environments. Basic information about the routes are given in Table 1. Visualization of individual routes, their environment and collected track logs is later presented in figures 3, 4 and 5.

Route n. 1 was set on the outskirts of the Opava city in the Czech Republic. The first third of the route is outside the built-up area with a minimally disturbed view of the sky. Then the route passes near low buildings and in some places also under the vegetation cover. Route n. 2 was situated in the campus of the VSB-Technical University of Ostrava. It includes two short underpasses with a complete blockage of the sky view. The area near the university's 35 m high rectorate building is also problematic (see Figure 2). The route here is directly connected to the first underpass and the sky view is also blocked from the other side by tree vegetation. In other parts, the route passes close to modern buildings, therefore in an environment with potential for high multipath effects.

Route n. 3 was located in the built-up area of the Ostrava city close to the university campus with the second route. The route starts and ends in a park surrounded by apartment buildings. Its large part can be considered as an urban canyon since it passes close to the sixteen-storey tower house or along the sidewalk adjacent to the six-story buildings (see Figure 2).

Table 1. Basic information about the three testing routes. Only turns where direction of movement changes for at least seventy degrees are being counted.

Route number	Length [km]	Number of turns	GNSS conditions
1	1.03	4	excellent to good
2	1.28	10	good to very poor
3	1.10	18	good to very poor

Data collection on the first route was realized during December, 2022 and on the two remaining routes in the beginning of January, 2023. Route n. 1 was driven a total of three times, the other two routes twice. The vehicle travel speed was around 5 km/h, corresponding to a standard speed of pedestrian walking. Before the start of the drive, the vehicle was always kept static for at least 10 minutes to ensure a proper initialization of the tested GNSS receivers. Starting points of all three routes were located in areas with a reasonable sky view and low probability of multipath.

Figure 2. Photos showing short sections of route n. 2 (top) and route n. 3 (bottom). Red line is indicating path travelled by the vehicle. Approximate location of the photo creation is shown on the map in Figure 4 or Figure 5, respectively.

2.3 Evaluation methodology

Route track logs from the u-blox module were exported to KML format containing individual waypoints recorded at an interval of 1 s. In the same format and form, route track logs from the

Samsung smartphone were also obtained from the Ultra GPS Logger application. Reference lines corresponding to the ground truth of driven routes were manually digitized based on several sources of data. In case of the route n. 1, mainly the aerial ortophotomosaic with a spatial resolution of 0.15 m was used. In case of the second and the third route, an official vector layer representing pavements in the Ostrava city was utilized. Moreover, a video record from camera installed on the vehicle itself was acquired during each drive and used to further edit the specific reference line representing the real position of vehicle during data collection. Accuracy of the reference lines is therefore between 0.1 to 0.2 m with a maximum deviation around 0.5 m potentially happening in several turnings.

U-blox module was positioned in the center of the vehicle while the smartphone was fixed at the side of vehicle. There was therefore an offset of 0.11 m between it and the u-blox module in the direction perpendicular to the movement of vehicle. To compensate this offset, reference lines were created individually for the u-blox module and for the smartphone.

To evaluate positioning performance of tested devices, horizontal distances between all individual points from their track logs and the corresponding reference line were computed and consequently statistically assessed.

Figure 3. Visualization of point track logs from the u-blox module (red) and from the Samsung smartphone (blue) together with the reference line (black). Route number 1, drive realized on December 9, 2022. Background map: OSM (https://www.openstreetmap.org/). Track logs from the other two drives on the route are comparable.

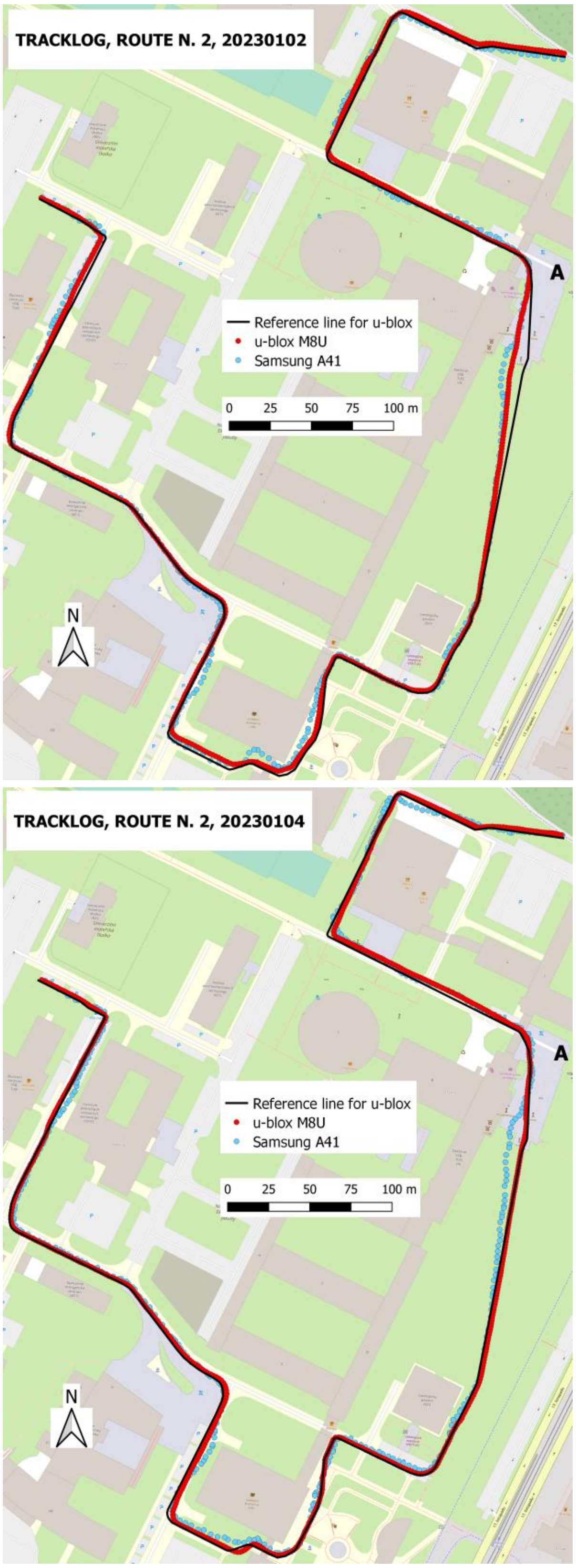

Figure 4. Visualization of point track logs from the u-blox module (red) and from the Samsung smartphone (blue) together with the reference line (black). Route number 2, drive realized on January 2, 2023 (top) and on January 4, 2023 (bottom). Letter "A" indicates an approximate location where photo shown in Figure 2 was taken. Background map: OSM (https://www.openstreetmap.org/).

m (2 m) and at the same time 24.8% of the points were at distances above 5 m. For the u-blox unit, the same parameters were 35.2%, 51.6% and 9.4%, respectively.

Number of points with a computed position was significantly lower from the smartphone compared to the u-blox device in all individual passes of all routes. As already mentioned, both devices were set to deliver output at 1s intervals. While the u-blox module was able to reliably provide localization at this interval, the Samsung A41 smartphone on average only provided a position every 1.7 s. The reason for this behaviour of the smartphone is likely due to the Ultra GPS Logger application used, which was unable to determine a position at each measurement epoch.

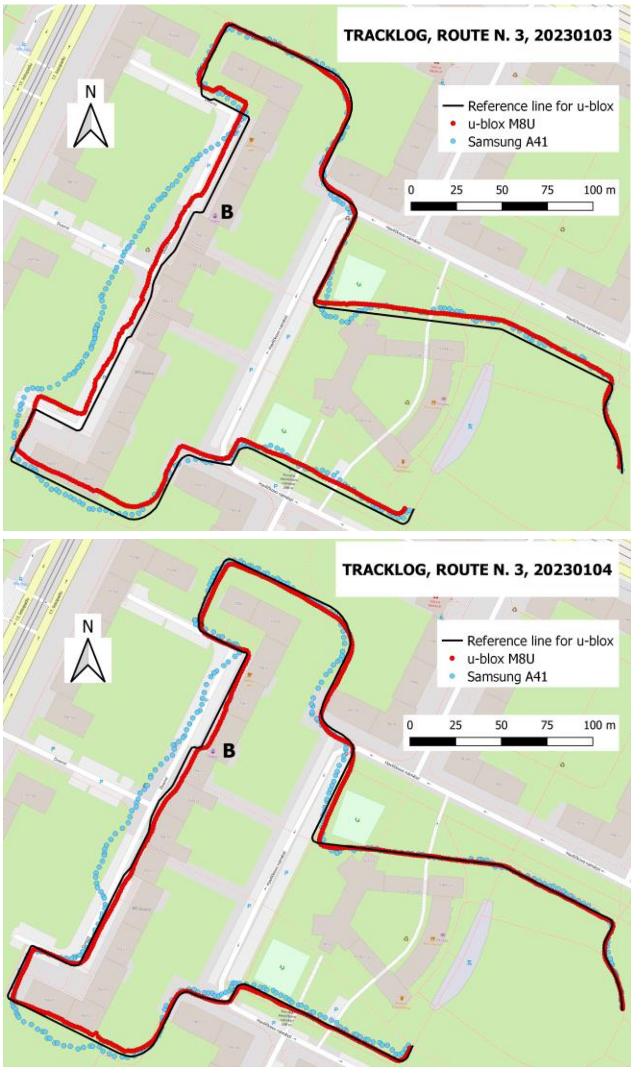

Figure 5. Visualization of point track logs from the u-blox module (red) and from the Samsung smartphone (blue) together with the reference line (black). Route number 3, drive realized on January 3, 2023 (top) and on January 4, 2023 (bottom). Letter "B" indicates an approximate location where photo shown in Figure 2 was taken. Background map: OSM (https://www.openstreetmap.org/).

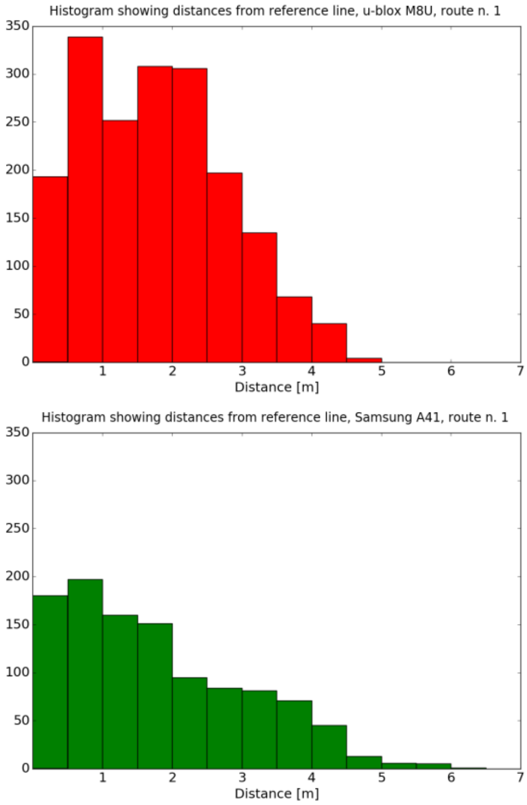

Figure 6. Histograms showing horizontal distances between points recorded by the tested devices and the reference line for route n. 1. U-blox M8U module shown in red color (top), Samsung A41 smartphone in green color (bottom).

3 RESULTS

Calculated horizontal distances between positions obtained by the tested devices and reference lines are displayed in a histogram (Figures 6 to 8) and categorised in Tables 2 to 4. The outputs show that higher positioning accuracy was achieved with the u-blox M8U. Although for the first route the results of both devices were comparable, for the second and third route in a purely urban environment, the advantages of the GNSS/INS fusion in the u-blox module were already evident, especially in terms of large positioning errors above 5 m. In case of the first route which offered the best environment for GNSS positioning, 34.6% (63.2%) of the smartphone points were within a distance of 1 m (2 m) from the reference line and only 1.1% of the points further than 5 m. For the u-blox unit, 28.9% (59.3%) of the points were within 1 m (2 m) and no points were in a distance exceeding 5 m. For the second route passing through the university campus, 28% (48.3%) of the points from the smartphone were within 1 m (2 m) and 8.7% of the points were further than 5 m. For the u-blox unit, the same parameters were 42.3%, 76.9% and 2.5%, respectively. In the case of the third route with the worst conditions for GNSS positioning, only 22.7% (43%) of the points from the smartphone were within 1

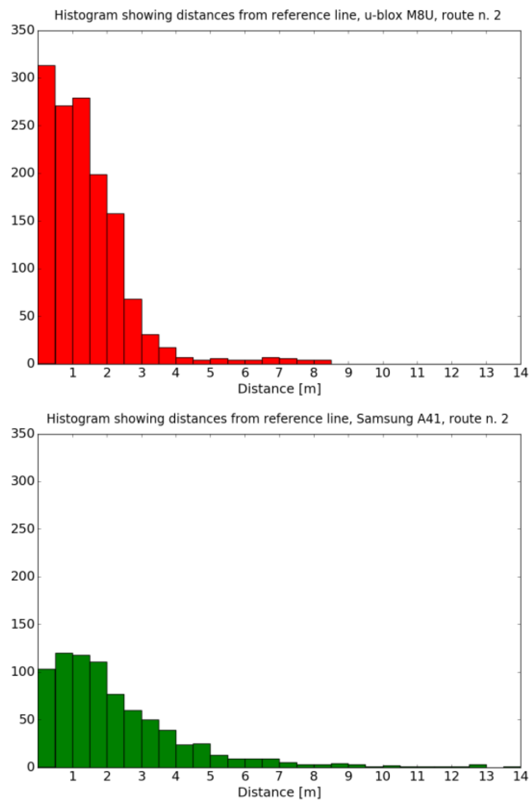

Figure 7. Histograms showing horizontal distances between points recorded by the tested devices and the reference line for route n. 2. U-blox M8U module shown in red color (top), Samsung A41 smartphone in green color (bottom).

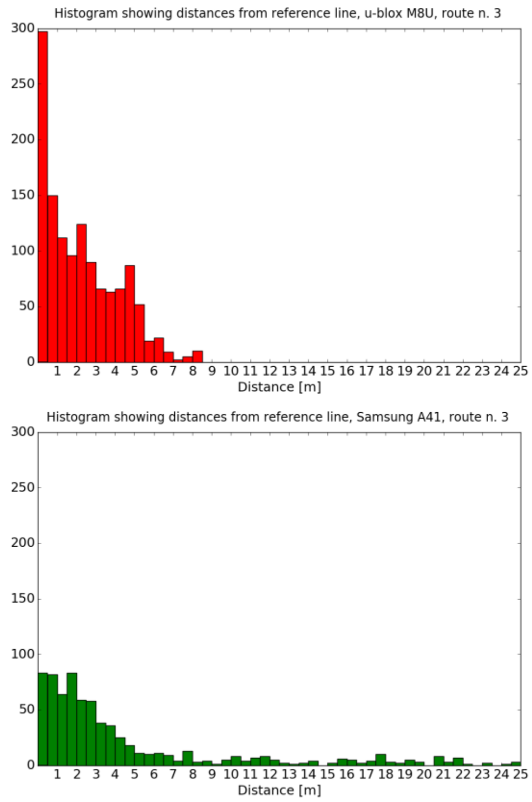

Figure 8. Histograms showing horizontal distances between points recorded by the tested devices and the reference line for route n. 3 . U-blox M8U module shown in red color (top), Samsung A41 smartphone in green color (bottom).

Interval of distances [m]	u-blox M8U	Samsung A41
0 – 0.24	136 (7.4 %)	100 (9.2 %)
0.25 – 0.49	57 (3.1 %)	80 (7.3 %)
0.5 – 0.99	339 (18.4 %)	197 (18.1 %)
1 – 1.99	560 (30.4 %)	311 (28.6 %)
2 – 2.99	503 (27.3 %)	179 (16.4 %)
3 – 3.99	203 (11.0 %)	152 (14.0 %)
4 – 4.99	44 (2.4 %)	58 (5.3 %)
5 – 9.99	0 (0 %)	12 (1.1 %)
10 – 19.99	0 (0 %)	0 (0 %)
> 20	0 (0 %)	0 (0 %)
Sum	**1842 (100 %)**	**1089 (100 %)**

Table 2. Horizontal distances between points recorded by the tested devices and the reference line classified to individual categories. Results for route n. 1 summarized from all three individual drives.

Interval of distances [m]	u-blox M8U	Samsung A41
0 – 0.24	145 (10.5 %)	51 (6.4 %)
0.25 – 0.49	168 (12.2 %)	52 (6.5 %)
0.5 – 0.99	271 (19.6 %)	120 (15.1 %)
1 – 1.99	478 (34.6 %)	229 (28.8 %)
2 – 2.99	226 (16.3 %)	137 (17.2 %)
3 – 3.99	48 (3.5 %)	89 (11.2 %)
4 – 4.99	11 (0.8 %)	49 (6.1 %)
5 – 9.99	35 (2.5 %)	59 (7.4 %)
10 – 19.99	0 (0 %)	10 (1.3 %)
> 20	0 (0 %)	0 (0 %)
Sum	**1382 (100 %)**	**796 (100 %)**

Table 3. Horizontal distances between points recorded by the tested devices and the reference line classified to individual categories. Results for route n. 2 summarized from all three individual drives.

Interval of distances [m]	u-blox M8U	Samsung A41
0 – 0.24	166 (13.1 %)	53 (7.3 %)
0.25 – 0.49	131 (10.3 %)	30 (4.1 %)
0.5 – 0.99	150 (11.8 %)	82 (11.3 %)
1 – 1.99	208 (16.4 %)	147 (20.3 %)
2 – 2.99	214 (16.8 %)	117 (16.1 %)
3 – 3.99	129 (10.2 %)	74 (10.2 %)
4 – 4.99	153 (12.0 %)	43 (5.9 %)
5 – 9.99	119 (9.4 %)	71 (9.8 %)
10 – 19.99	0 (0 %)	83 (11.5 %)
> 20	0 (0 %)	25 (3.5 %)
Sum	**1270 (0 %)**	**725 (100 %)**

Table 4. Horizontal distances between points recorded by the tested devices and the reference line classified to individual categories. Results for route n. 3 summarized from all three individual drives.

Results of statistical evaluation computed from horizontal distances between points provided by the tested devices and reference lines are provided in Table 5. Mean horizontal distance for the u-blox M8U device varied between 1.2 and 2.0 m, except for one pass of route n. 3, when it reached 3.3 m. The standard deviation (SDEV) of distances from the reference line varied between 0.8 and 1.2 m, except for one pass of route n. 2 (1.6 m) and one pass of route n. 3 (2.1 m). In case of route n. 1, all three passes were very similar in terms of achieved values of the statistical parameters. For the remaining two routes, the results of the two passes differed from each other, with one of them always providing visibly better results in terms of mean distance and standard deviation. This situation was due to a less accurate positioning in the most problematic parts of the routes during one of the passes, as can be seen in Figures 4 and 5. Although the tracklogs from the u-blox module are represented by smooth lines without a scattering apparent in the smartphone outputs, in areas with very limited sky view or complete sky obscuration the absolute positioning can be significantly degraded.

On the route n. 1, Samsung A41 smartphone achieved rather similar mean distances as the u-blox unit, however its standard deviations were about 20 to 40% higher. For routes 2 and 3, both mean distances and SDEVs were higher by tens or even hundreds of %. Map outputs shown in Figure 4 and 5 evince that especially in an environment with poor sky visibility, the smartphone using only GNSS technology had significant issues with maintaining quality of the position estimation.

Table 5. Statistical parameters calculated from horizontal distances between the route points recorded by the test devices and the reference line for individual route passes. Date format: YYMMDD, AM = morning, PM = afternoon; Device: S = Samsung A41, U = u-blox M8U.

Route n.	Date	Device	Mean (m)	SDEV (m)	Max (m)	Samples
1	221209 PM	S	1.77	1.21	4.56	367
	221229 AM	S	1.57	1.21	5.61	359
	221229 PM	S	2.00	1.41	6.04	363
	221209 PM	U	1.42	0.98	3.44	634
	221229 AM	U	1.96	0.86	3.89	604
	221229 PM	U	1.93	1.18	4.69	604
2	230102 PM	S	2.39	2.37	13.54	374
	230104 AM	S	2.23	1.75	11.16	422
	230102 PM	U	1.71	1.55	8.48	649
	230104 AM	U	1.15	0.78	3.30	733
3	230103 PM	S	5.84	6.69	24.95	354
	230104 AM	S	3.39	3.75	17.47	371
	230103 PM	U	3.26	2.07	8.44	623
	230104 AM	U	1.31	0.99	4.28	647

4 CONCLUSIONS

In this paper, we have evaluated a positioning performance of the low-cost u-blox M8U module in scenarios simulating movement of a pedestrian or some low speed vehicle in an urban environment. The tested u-blox module is primarily aimed on automotive industry applications and fusing the GNSS and INS outputs into a combined solution requires a realization of initialization and calibration drive. Since exceeding speeds of 40 to 50 km/h is necessary during the initialization and calibration drive, it must be performed on a vehicle allowing such a travel speed. In our case, the drive was made with a standard passenger car with the device fixed on its roof. After this procedure, the module was smoothly operating in the fused UDR mode on our four-wheeled remotely controlled vehicle at speeds around 5 km/h.

A series of testing drives on three individual routes in various environments was done to study the positioning performance and behavior. According to their summary results, the accuracy of horizontal position of the u-blox M8U module was in 35% of all measurements better than 1 m and in 84% better than 3 m. The positioning error exceeded 5 m only in 3.4% of all measurements and the maximum reached value was 8.5 m. The simultaneously tested Samsung A41 smartphone equipped only with a single-frequency multi-GNSS receiver provided an accuracy of horizontal positioning better than 1 m in 29% of all measurements and an accuracy better than 3 m in 72%. It is necessary to note that large errors were more common for this device with 9.1% of all measurements exceeding 5 m and the maximum value reaching 25 m. We find the performance achieved by the tested smartphone to be expectable given its hardware and the characteristics of the performed tests. The u-blox module performed visibly better in areas with a very limited or completely blocked view over the sky, therefore in places where the module had the advantage of an input from the inertial unit.

As above mentioned, [Feng 2020] included the u-blox M8U module as a reference in their evaluation of own developed deeply-coupled integration of GNSS and INS. They realized 30 minutes long testing drive in an urban environment of the Wuhan city in China using a passenger car. In latitude and longitude, the u-blox M8U module in the GNSS/INS fusion mode achieved standard deviation at the level of 3 to 4 m. The maximum error was 11.6 m, found in the longitude. Since no other study utilizing the u-blox M8U receiver was found, our results can be further compared only with works based on different (low-cost) devices. In [Gonzalez 2019], root mean square error (RMSE) of 6.4 m in latitude and 10.6 m in longitude was reached in vehicular test on the streets of the city of Turin with an own implementation of loosely-coupled integration based on a single-frequency u-blox M8T GNSS receiver and MEMS INS. The positioning performance achieved in our study was better than that of the two mentioned studies. Some positive impact on it might came from collecting the data during a non-growing season when vegetation is without leaves. Still, a much higher horizontal accuracy of GNSS/INS integration is achievable with RMSE around 0.1 to 0.2 m as presented by [Gao 2018]. However, they used a good quality Trimble BD982 dual-frequency GNSS receiver with a PPP solution. The multi-GNSS PPP solution itself without an input from the INS reached an accuracy of about 0.2 to 0.3 m. A decimeter level accuracy of GNSS/INS integration was reported also by [Zhao 2016], however their solution was based on RTK technique and not specified type of GPS receiver. Despite the tested u-blox M8U module cannot provide such a level of performance, its distinct advantage is its low cost and simplicity as it does not require any external data or (post)-processing as the mentioned RTK or PPP techniques. For urban low speed applications where an accuracy of 2-3 m in real time is sufficient and where occasional higher deviations can be tolerated, it represents a solution which can be easily implemented and used.

ACKNOWLEDGMENTS

The work was co-financed from the state budget by the Technology agency of the Czech Republic under the Doprava2020+ Programme, the project CK01000190 „Sensor measurements of urban footways to support mobility of disabled people", and supported by the European Regional

Development Fund in the Research Centre of Advanced Mechatronic Systems project, CZ.02.1.01/0.0/0.0/16_019/0000867 within the Operational Programme Research, Development, and Education.

REFERENCES

[Abbott 2003] Abbott, A.S. and Lillo, W.E. Global Positioning Systems and Inertial Measuring Unit Ultratight Coupling Method. US Patent No. 6516021, 4 February 2003.

[Aggarwal 2010] Aggarwal, P. et al. MEMS-Based Integrated Navigation. Artech House Publisher, Norwood, UK, 2010.

[Agrisano 2012] Agrisano, A. et al. Benefits of Combined GPS/GLONASS with Low-Cost MEMS IMUs for Vehicular Urban Navigation. Sensors, 2012, Vol. 12. doi:10.3390/s120405134.

[Basso 2020] Basso, M. et al. Triggered INS/GNSS Data Fusion Algorithms for Enhanced Pedestrian Navigation System. IEEE Sensors Journal, 2020, Vol. 20, pp. 7447-7459. doi: 10.1109/JSEN.2020.2979335.

[Biagi 2016] Biagi, L. et al. Low-Cost GNSS Receivers for Local Monitoring: Experimental Simulation, and Analysis of Displacements. Sensors, 2016, Vol. 16. doi:10.3390/s16122140.

[Chiang 2020] Chiang, K.-W. et al. Assessment for INS/GNSS/Odometer/Barometer Integration in Loosely-Coupled and Tightly-Coupled Scheme in a GNSS-Degraded Environment. IEEE Sensors Journal, 2020, Vol. 20, pp. 3057–3069. doi:10.1109/JSEN.2019.2954532.

[De Gaetani 2019] De Gaetani et al. Improving Low-Cost GNSS Navigation in Urban Areas by Integrating a Kinect Device. International Association of Geodesy Symposia, 2019, Vol. 149, pp. 183-189. doi:10.1007/1345_2018_27.

[Dietmayer 2005] Dietmayer, K., et al. Roadway detection and lane detection using multilayer laserscanner. Advanced Microsystems for Automotive Applications. Springer: New York, USA, 2005.

[Falco 2017] Falco, G., et al. Loose and Tight GNSS/INS Integrations: Comparison of Performance Assessed in Real Urban Scenarios. Sensors, 2017, Vol. 17. doi:10.3390/s17020255.

[Feng 2013] Feng, Q. et al. Performance improvement of receivers based on ultra-tight integration in GNSS-challenged environments. Sensors, 2013, Vol. 13. doi: 10.3390/s131216406.

[Feng 2020] Feng, X., et al. Implementation and Performance of a Deeply-Coupled GNSS Receiver with Low-Cost MEMS Inertial Sensors for Vehicle Urban Navigation. Sensors, 2020, Vol. 20. doi:10.3390/s20123397.

[Garrido-Carretero 2019] Garrido-Carretero, M.S., et al. Low-cost GNSS receiver in RTK positioning under the standard ISO-17123-8: A feasible option in geomatics. Measurement, 2019, Vol. 137, pp. 168–178. doi: 10.1016/j.measurement.2019.01.045.

[Gao 2015] Gao, Y., et al. INS/GPS/LiDAR Integrated Navigation System for Urban and Indoor Environments Using Hybrid Scan Matching Algorithm. Sensors, 2015, Vol. 15, pp. 23286–23306. doi:10.3390/s150923286.

[Gao 2018] Gao, Z., et al. Odometer, low-cost inertial sensors, and four-GNSS data to enhance PPP and attitude determination. GPS Solutions, 2018, Vol. 22. doi:10.1007/s10291-018-0725-y.

[Gonzales 2019] Gonzales, R. and Dabove, P. Performance Assessment of an Ultra Low-Cost Inertial Measurement Unit for Ground Vehicle Navigation. Sensors, 2019, Vol. 19. doi:10.3390/s19183865.

[Groves 2019] Groves, P. and Adjard, M. Performance assessment of 3D-mapping–aided GNSS part 1: Algorithms, user equipment, and review. Navigation, Journal of the Institute of Navigation, 2019, Vol. 66, pp. 341-362. doi:10.1002/navi.288.

[Hamza 2021] Hamza, V. et al. Testing the Performance of Multi-Frequency Low-Cost GNSS Receivers and Antennas. Sensors, 2021, Vol. 21. doi:10.3390/s21062029.

[Hsu 2016] Hsu, L.-T., et al. 3D building model-based pedestrian positioning method using GPS/GLONASS/QZSS and its reliability calculation. GPS Solutions, 2016, Vol. 20, pp. 413-428, doi:10.1007/s10291-015-0451-7.

[Janos 2022] Janos, D., et al. Evaluation of low-cost RTK GNSS receiver in motion under demanding conditions. Measurement, 2022, Vol. 201. doi:10.1016/j.measurement.2022.111647.

[Javed 2022] Javed, A.R., et al. Future smart cities requirements, emerging technologies, applications, challenges, and future aspects. Cities, 2022, Vol. 129. doi:10.1016/j.cities.2022.103794.

[Kaczmarek 2022] Kaczmarek, A., et al. Experimental 2D extended Kalman filter sensor fusion for low-cost GNSS/IMU/Odometers precise positioning system. Measurement, 2022, Vol. 193. doi:10.1016/j.measurement.2022.110963.

[Kubo 2016] Kubo, N., and Suzuki, T. Performance improvement of RTK-GNSS with IMU and vehicle speed sensors in an urban environment. IEICE Transactions on Fundamentals of Electronics, Communications and Computer Sciences, 2016, Vol. E99A, pp. 217-224. doi:10.1587/transfun.E99.A.217.

[Le Scornec 2017] Le Scornec, J., et al. Foot-mounted pedestrian navigation reference with tightly coupled GNSS carrier phases, inertial and magnetic data. International Conference on Indoor Positioning and Indoor Navigation, Sapporo Japan, September 18-21, 2017. doi:10.1109/IPIN.2017.8115882.

[Li 2017] Li, T., et al. Tightly-Coupled Integration of Multi-GNSS Single-Frequency RTK and MEMS-IMU for Enhanced Positioning Performance. Sensors, 2017, Vol. 17. doi:10.3390/s17112462.

[Li 2018] Li, T., et al. High-Accuracy Positioning in Urban Environments Using Single-Frequency Multi-GNSS RTK/MEMSIMU Integration. Remote Sensing, 2018, Vol. 10. doi:10.3390/rs10020205.

[Li 2019] Li, T., et al. Tight fusion of a monocular camera, mems-imu, and single-frequency multi-gnss rtk for precise navigation in gnss-challenged environments. Remote Sensing, 2019, Vol. 11. doi:10.3390/rs11060610.

[Lyu 2020] Lyu, Z., and Gao, Y. An SVM Based Weight Scheme for Improving Kinematic GNSS Positioning Accuracy with Low-Cost GNSS Receiver in Urban Environments. Sensors, 2020, Vol. 20. doi:10.3390/s20247265.

[Maddikunta 2022]Maddikunta, P.K.R., et al. Industry 5.0: A survey on enabling technologies and potential applications. Journal of Industrial Information

Integration, 2022, Vol. 26. doi:10.1016/j.jii.2021.100257.
[Niesen 2018] Niesen, U., et al. Accurate positioning in GNSS-challenged environments with consumer-grade sensors. Proceedings of the 31st International Technical Meeting of the Satellite Division of the Institute of Navigation, ION GNSS+ 2018, Florida, USA, September 24-28, 2018. doi:10.33012/2018.15998.
[Notti 2020] Notti, D., et al. Low-Cost GNSS solution for continuous monitoring of slope instabilities applied to Madonna Del Sasso Sanctuary (NW Italy). Sensors, 2020, Vol. 20. doi:10.3390/s20010289.
[Odolinski 2017] Odolinski, R. and Teunissen, P. Low-cost, high-precision, single-frequency GPS–BDS RTK positioning. GPS Solutions, 2017, Vol. 21, pp. 1315-1330. doi:10.1007/s10291-017-0613-x.
[Pany 2009] Pany, T., et al. Performance of a partially coherent ultra-tightly coupled GNSS/INS pedestrian navigation system enabling coherent integration times of several seconds to track GNSS signals down to 1.5 dBHz. 22nd International Technical Meeting of the Satellite Division of the Institute of Navigation 2009, ION GNSS 2009, Savannah, USA, September 22-25, 2009.
[Park 2008] Park, M. and Gao, Y. Error and performance analysis of MEMS-based inertial sensors with a low-cost GPS receiver. Sensors, 2008, Vol. 8, pp. 2240-2261. doi:10.3390/s8042240.
[Petovello 2003] Petovello, M. Real-time Integration of a Tactical-Grade IMU and GPS for High-Accuracy Positioning and Navigation. Ph.D. Thesis, University of Calgary, Calgary, Canada, 2003.
[Rademakers 2016] Rademakers E., et al. Obtaining real-time sub-meter accuracy using a low cost GNSS device. 2016 European Navigation Conference, ENC 2016, Helsinki, Finland, May 30 – June 2, 2016. doi:10.1109/EURONAV.2016.7530555.
[Shaeffer 2013] Shaeffer, D. MEMS inertial sensors: A tutorial overview. IEEE Communications Magazine, 2013, Vol. 51, pp. 100-109. doi:10.1109/MCOM.2013.6495768.
[Solimeno 2007] Solimeno, A. Low-Cost INS/GPS Data Fusion with Extended Kalman Filter for Airborne Applications. Master's Thesis, Universidad Tecnica de Lisboa, Lisbon, Portugal, 2007.
[Šegina 2020] Šegina, E., et al. Monitoring surface displacement of a deep-seated landslide by a low-cost and near real-time GNSS system. Remote Sensing, 2020, Vol. 12, pp. 1–26. doi:10.3390/rs12203375.
[Teunissen 2017] Teunissen, P.J.G. and Montenbruck, O. (eds.). Springer Handbook of Global Navigation Satellite Systems. Springer International Publishing, 2017. ISBN 978-3-319-42926-7. doi:10.1007/978-3-319-42928-1.
[Toledo-Moreo 2007] Toledo-Moreo, R., et al. High-integrity IMM-EKF-based road vehicle navigation with low-cost GPS/SBAS/INS. IEEE Transactions on Intelligent Transportation Systems, 2007, Vol. 8, pp. 491–511. doi:10.1109/TITS.2007.902642.
[u-blox 2021] u-blox. u-blox 8 / u-blox M8 Receiver description, Including protocol specification. UBX-13003221 - R26, U-blox AG: Thalwil, Switzerland, 2021.
[Vivacqua 2017] Vivacqua, R., et al. A Low Cost Sensors Approach for Accurate Vehicle Localization and Autonomous Driving Application. Sensors, 2017, Vol. 17. doi:10.3390/s17102359.
[Wielgocka 2021] Wielgocka, N., et al. Feasibility of Using Low-Cost Dual-Frequency GNSS Receivers for Land Surveying. Sensors, 2021, Vol. 21. doi: 10.3390/s21061956.
[Xu 2020] Xu, H., et al. Machine learning based LOS/NLOS classifier and robust estimator for GNSS shadow matching. Satellite Navigation, 2020, Vol. 1. doi:10.1186/s43020-020-00016-w.
[Zhao 2016] Zhao, S., et al. High-Precision Vehicle Navigation in Urban Environments Using an MEM's IMU and Single-Frequency GPS Receiver. IEEE Transactions on Intelligent Transportation Systems, 2016, Vol. 17, pp. 2854-2867. doi:10.1109/TITS.2016.2529000.
[Zumberge 1997] Zumberge, J.F., et al. Precise point positioning for the efficient and robust analysis of GPS data from large networks. Journal of Geophysical Research: Solid Earth, 1997, Vol. 102, pp. 5005–5017. doi: 10.1029/96JB03860.

CONTACTS:

doc. Ing. Michal Kacmarik, Ph.D.
VSB - Technical University of Ostrava, Department of geoinformatics
17. listopadu 2172/15, Ostrava-Poruba, 708 00, Czech Republic
+420 596 995 512, michal.kacmarik@vsb.cz
https://www.hgf.vsb.cz/548/en/

Ing. David Fojtik, Ph.D.
VSB - Technical University of Ostrava, Department of Control Systems and Instrumentation
17. listopadu 2172/15, Ostrava-Poruba, 708 00, Czech Republic
+420 596 994 193, david.fojtik@vsb.cz
https://www.fs.vsb.cz/352/en/